LMS AND NLMS ALGORITHMS FOR THE IDENTIFICATION OF IMPULSE RESPONSES WITH INTRINSIC SYMMETRIC OR ANTISYMMETRIC PROPERTIES

Jacob Benesty[*], *Constantin Paleologu*[†], *Silviu Ciochină*[†],
Eduardo Vinicius Kuhn[‡], *Khaled Jamal Bakri*[‡], *and Rui Seara*[‡]

[*]INRS-EMT, University of Quebec, Montreal, Canada, e-mail: jacob.benesty@inrs.ca
[†]Polytechnic University of Bucharest, Romania, e-mail: {pale, silviu}@comm.pub.ro
[‡]Federal University of Santa Catarina, Florianópolis, Brazil, e-mail: {kuhn, khaled, seara}@linse.ufsc.br

ABSTRACT

In applications involving system identification problems, some characteristics of the impulse response of the system to be identified are usually exploited to design adaptive algorithms with improved performance. In this context, this paper focuses on the identification of systems that own intrinsic symmetric or antisymmetric properties, which can be further formulated by using a combination of bilinear forms. Based on such an approach, the least-mean-square (LMS) and normalized LMS (NLMS) algorithms with symmetric/antisymmetric properties (termed here LMS-SAS and NLMS-SAS) are proposed. Simulation results are shown confirming the improved convergence speed achieved by the proposed algorithms as compared to the conventional LMS and NLMS counterparts for different operating scenarios.

***Index Terms*—** Adaptive filters, bilinear forms, least-mean-square algorithm, symmetric and antisymmetric impulse responses, system identification, Kronecker product decomposition.

1. INTRODUCTION

Adaptive filtering techniques used in system identification problems [1–4] typically exploit intrinsic characteristics of the impulse responses of the system to be identified (unknown system), aiming to improve the performance of the adaptive algorithm. For example, sparse adaptive filters are designed to exploit the sparseness of the impulse responses in specific applications, such as echo cancellation [5–8]. Also, tensor-based algorithms can be used for the identification of linearly separable systems [9, 10]. Such tensorial approaches are involved in applications like source separation [11, 12], array beamforming [13, 14], and object recognition [15, 16]. The basic idea behind the tensorial adaptive filters relies on the modeling techniques of rank-1 tensors (or multilinear forms), exploiting the Kronecker product decomposition of the global impulse response. Note that bilinear forms represent the special case of a two-dimensional Kronecker decomposition [17–19].

In this context, [20] has recently targeted the identification of impulse responses with intrinsic symmetric or antisymmetric properties using bilinear forms. Specifically, the solution presented in [20] leads to an iterative Wiener filter, exhibiting enhanced performance (as compared with the conventional Wiener filter) especially when a small amount of data is available for the estimation of the required statistics. Therefore, based on [20], we proceed further by proposing here the least-mean-square (LMS) and the normalized LMS (NLMS) algorithms with intrinsic symmetric or antisymmetric properties, without claiming to cover any particular application. This paper focuses on the capabilities and features of the algorithms for a general framework of system identification aiming to provide a theoretical benchmark.

The remainder of the paper is organized as follows. Section 2 introduces the system model and revisits the LMS and NLMS algorithms. The proposed algorithms are developed in Section 3. Simulation results are provided in Section 4. Finally, conclusions are summarized in Section 5, while Section 6 outlines the relation to prior research works.

Throughout this paper, the adopted mathematical notation follows the standard practice of using lower-case boldface letters for vectors, upper-case boldface letters for matrices, and both italic Roman and Greek letters for scalar quantities. Superscript T stands for the transpose of a matrix, $\otimes$ denotes the Kronecker product [21], $\mathrm{vec}(\cdot)$ characterizes the vectorization operation, $\mathrm{Tr}(\cdot)$ represents the trace of a square matrix, and $||\cdot||$ is the Euclidean norm. Note that this study focuses on real-valued and zero-mean (input, output, and noise) signals.

2. PROBLEM FORMULATION

This section presents the considered system model and revisits the conventional LMS and NLMS algorithms.

2.1. System model

Let us consider a linear single-input/single-output (SISO) system, whose output signal (defined also as desired signal) at a discrete-time index k is given by

$$\begin{aligned} d(k) &= \overline{\mathbf{h}}^{\mathrm{T}}\left(\mathbf{h}_1, \mathbf{h}_2\right)\mathbf{x}(k) + w(k) \\ &= y(k) + w(k) \end{aligned} \tag{1}$$

where $\overline{\mathbf{h}}\left(\mathbf{h}_1, \mathbf{h}_2\right)$ is the system impulse response of length $L = L_0^2$, which depends on the two sub-impulse responses $\mathbf{h}_1$ and $\mathbf{h}_2$ of length L_0, the vector $\mathbf{x}(k) = [x(k)\ x(k-1)\ \ldots\ x(k-L+1)]^{\mathrm{T}}$ contains the L most recent samples of the input signal $x(k)$, and $w(k)$ characterizes the additive noise.

Now, let us assume that the system impulse response is of the following type:

$$\overline{\mathbf{h}}\left(\mathbf{h}_1, \mathbf{h}_2\right) = \mathbf{h}_1 \otimes \mathbf{h}_2 \pm \mathbf{h}_2 \otimes \mathbf{h}_1. \tag{2}$$

This research work was supported in part by the Brazilian National Council for Scientific and Technological Development (CNPq) and by the Ministry of Education and Research, Romania, CNCS - UEFISCDI, project number PN-III-P1-1.1-TE-2019-0529, within PNCDI III.

So, the impulse response is symmetric if

$$\overrightarrow{\mathbf{h}}\,(\mathbf{h}_1,\mathbf{h}_2)=\mathbf{h}_1\otimes\mathbf{h}_2+\mathbf{h}_2\otimes\mathbf{h}_1 \tag{3}$$

and antisymmetric if

$$\overleftarrow{\mathbf{h}}\,(\mathbf{h}_1,\mathbf{h}_2)=\mathbf{h}_1\otimes\mathbf{h}_2-\mathbf{h}_2\otimes\mathbf{h}_1. \tag{4}$$

When the system impulse response is symmetric, the following relations hold:

$$\begin{aligned}\overrightarrow{\mathbf{h}}\,(\mathbf{h}_1,\mathbf{h}_2)&=\overrightarrow{\mathbf{h}}\,(\mathbf{h}_2,\mathbf{h}_1)\\ \overrightarrow{\mathbf{h}}\,(\mathbf{h}_1,\mathbf{h}_1)&=2\,(\mathbf{h}_1\otimes\mathbf{h}_1)\end{aligned} \tag{5}$$

and when the system impulse response is antisymmetric

$$\begin{aligned}\overleftarrow{\mathbf{h}}\,(\mathbf{h}_1,\mathbf{h}_2)&=-\overleftarrow{\mathbf{h}}\,(\mathbf{h}_2,\mathbf{h}_1)\\ \overleftarrow{\mathbf{h}}\,(\mathbf{h}_1,\mathbf{h}_1)&=\mathbf{0}_L\end{aligned} \tag{6}$$

with $\mathbf{0}_L$ denoting an L-dimensional column vector of 0's. In both cases, we have that $\overline{\mathbf{h}}\,(\mathbf{h}_1,\mathbf{h}_2+\mathbf{h}_3)=\overline{\mathbf{h}}\,(\mathbf{h}_1,\mathbf{h}_2)+\overline{\mathbf{h}}\,(\mathbf{h}_1,\mathbf{h}_3)$, where $\mathbf{h}_1$, $\mathbf{h}_2$, and $\mathbf{h}_3$ are three sub-impulse responses of length L_0. Note that the symmetric/antisymmetric characteristic considered here is not related to the samples of the impulse response (such as in linear-phase finite impulse response filters), but to the mathematical definitions (3)–(6).

Finally, taking into account (2), the term $y(k)$ in (1) can be rewritten as

$$\begin{aligned}d(k)&=(\mathbf{h}_1\otimes\mathbf{h}_2\pm\mathbf{h}_2\otimes\mathbf{h}_1)^{\mathrm{T}}\mathbf{x}(k)+w(k)\\ &=[\mathrm{vec}^{\mathrm{T}}(\mathbf{h}_2\mathbf{h}_1^{\mathrm{T}})\pm\mathrm{vec}^{\mathrm{T}}(\mathbf{h}_1\mathbf{h}_2^{\mathrm{T}})]\mathrm{vec}[\mathbf{X}(k)]+w(k)\\ &=\mathrm{Tr}[(\mathbf{h}_2\mathbf{h}_1^{\mathrm{T}})^{\mathrm{T}}\mathbf{X}(k)]\pm\mathrm{Tr}[(\mathbf{h}_1\mathbf{h}_2^{\mathrm{T}})^{\mathrm{T}}\mathbf{X}(k)]+w(k)\\ &=\mathbf{h}_2^{\mathrm{T}}\mathbf{X}(k)\mathbf{h}_1\pm\mathbf{h}_1^{\mathrm{T}}\mathbf{X}(k)\mathbf{h}_2+w(k)\end{aligned} \tag{7}$$

where[1]

$$\mathbf{X}(k)=[\mathbf{x}_0(k)\ \ \mathbf{x}_0(k-L_0)\ \ \ldots\ \ \mathbf{x}_0(k-(L_0-1)L_0)] \tag{8}$$

denotes a matrix of size $L_0\times L_0$ whose columns are given by

$$\mathbf{x}_0(k)=[x(k)\ \ x(k-1)\ \ldots\ x(k-L_0+1)]^{\mathrm{T}}. \tag{9}$$

Notice that (7) involves the sum of two bilinear forms in $\mathbf{h}_1$ and $\mathbf{h}_2$ [17].

2.2. Revisiting the LMS and NLMS algorithms

In the LMS algorithm, the update rule used for adjusting an L-dimensional adaptive weight vector $\widehat{\mathbf{h}}(k)$ is given by [4]

$$\widehat{\mathbf{h}}(k)=\widehat{\mathbf{h}}(k-1)+\mu\mathbf{x}(k)e(k) \tag{10}$$

where $0<\mu<2/(L\sigma_x^2)$ is the step-size parameter (with σ_x^2 being the variance of the input signal) and

$$e(k)=d(k)-\widehat{\mathbf{h}}^{\mathrm{T}}(k-1)\mathbf{x}(k) \tag{11}$$

defines the error signal. In turn, the update rule of the NLMS algorithm can be expressed as [4]

$$\widehat{\mathbf{h}}(k)=\widehat{\mathbf{h}}(k-1)+\frac{\alpha\mathbf{x}(k)e(k)}{\mathbf{x}^{\mathrm{T}}(k)\mathbf{x}(k)+\delta} \tag{12}$$

[1]Note from (8) and (9) that $\mathbf{x}(k)$ [in (1)] is obtained by stacking all columns of $\mathbf{X}(k)$, i.e., $\mathbf{x}(k)=\mathrm{vec}[\mathbf{X}(k)]$.

with $0<\alpha<2$ denoting the normalized step-size parameter and $\delta>0$ being the regularization parameter [22]. Nevertheless, although these algorithms may be used to identify $\overline{\mathbf{h}}(\mathbf{h}_1,\mathbf{h}_2)$ directly from (1), it is important to highlight that (10) and (12) involve the estimation of a impulse response of length $L=L_0^2$, which could be quite expensive in terms of the number of multiplications and additions. Moreover, this direct approach does not take into account any symmetry or antisymmetry constraint on the system impulse response. Therefore, our main goal here is to propose an efficient solution based on (7), where only $2L_0$ weights need to be estimated and the symmetry or antisymmetry constraint is considered.

3. PROPOSED ALGORITHMS

Here, the identification problem involving $\overline{\mathbf{h}}(\mathbf{h}_1,\mathbf{h}_2)$ is first reformulated, which then leads us to derive the proposed algorithms.

3.1. Reformulating the identification problem

Instead of estimating $\overline{\mathbf{h}}(\mathbf{h}_1,\mathbf{h}_2)$ directly, let us now assume that $\mathbf{h}_1$ and $\mathbf{h}_2$ [in (2)] can be identified by using two adaptive filters (both of length L_0) with weight vectors $\widehat{\mathbf{h}}_1(k)$ and $\widehat{\mathbf{h}}_2(k)$, respectively, in such a way that

$$\widehat{\overline{\mathbf{h}}}(k)=\widehat{\mathbf{h}}_1(k)\otimes\widehat{\mathbf{h}}_2(k)\pm\widehat{\mathbf{h}}_2(k)\otimes\widehat{\mathbf{h}}_1(k) \tag{13}$$

represents an estimate of $\overline{\mathbf{h}}(\mathbf{h}_1,\mathbf{h}_2)$. Alternatively, (13) can be expressed as

$$\widehat{\overline{\mathbf{h}}}(k)=\overline{\mathbf{H}}_{\widehat{\mathbf{h}}_2}(k)\widehat{\mathbf{h}}_1(k) \tag{14}$$

and

$$\widehat{\overline{\mathbf{h}}}(k)=\overline{\mathbf{H}}_{\widehat{\mathbf{h}}_1}(k)\widehat{\mathbf{h}}_2(k) \tag{15}$$

in which

$$\overline{\mathbf{H}}_{\widehat{\mathbf{h}}_2}(k)=\mathbf{I}_{L_0}\otimes\widehat{\mathbf{h}}_2(k)\pm\widehat{\mathbf{h}}_2(k)\otimes\mathbf{I}_{L_0} \tag{16}$$

and

$$\overline{\mathbf{H}}_{\widehat{\mathbf{h}}_1}(k)=\widehat{\mathbf{h}}_1(k)\otimes\mathbf{I}_{L_0}\pm\mathbf{I}_{L_0}\otimes\widehat{\mathbf{h}}_1(k) \tag{17}$$

characterize matrices of size $L\times L_0$. Therefore, from (14) and (15), the error signal (11) can be rewritten in two alternative ways, i.e.,

$$e(k)=d(k)-\widehat{\mathbf{h}}_1^{\mathrm{T}}(k-1)\mathbf{x}_2(k) \tag{18}$$

and

$$e(k)=d(k)-\widehat{\mathbf{h}}_2^{\mathrm{T}}(k-1)\mathbf{x}_1(k) \tag{19}$$

where

$$\mathbf{x}_2(k)=\overline{\mathbf{H}}_{\widehat{\mathbf{h}}_2}^{\mathrm{T}}(k-1)\mathbf{x}(k) \tag{20}$$

and

$$\mathbf{x}_1(k)=\overline{\mathbf{H}}_{\widehat{\mathbf{h}}_1}^{\mathrm{T}}(k-1)\mathbf{x}(k). \tag{21}$$

3.2. LMS algorithm with symmetric/antisymmetric properties

Now, following a bilinear optimization strategy [17], [18], the proposed LMS algorithm with symmetric/antisymmetric properties (termed here LMS-SAS) can be derived from (18) and (19). Specifically, from (18) and assuming that $\widehat{\mathbf{h}}_2(k)$ is fixed, the update rule of the first adaptive filter $\widehat{\mathbf{h}}_1(k)$ is obtained as

$$\begin{aligned}\widehat{\mathbf{h}}_1(k)&=\widehat{\mathbf{h}}_1(k-1)-\frac{\mu_1}{2}\frac{\partial[d(k)-\widehat{\mathbf{h}}_1^{\mathrm{T}}(k-1)\mathbf{x}_2(k)]^2}{\partial\widehat{\mathbf{h}}_1(k-1)}\\ &=\widehat{\mathbf{h}}_1(k-1)+\mu_1\mathbf{x}_2(k)e(k)\end{aligned} \tag{22}$$

while, using (19) and assuming that $\widehat{\mathbf{h}}_1(k)$ is fixed, the update rule for the second adaptive filter $\widehat{\mathbf{h}}_2(k)$ becomes

$$\begin{aligned}\widehat{\mathbf{h}}_2(k) &= \widehat{\mathbf{h}}_2(k-1) - \frac{\mu_2}{2}\frac{\partial[d(k)-\widehat{\mathbf{h}}_2^{\mathrm{T}}(k-1)\mathbf{x}_1(k)]^2}{\partial\widehat{\mathbf{h}}_2(k-1)} \\ &= \widehat{\mathbf{h}}_2(k-1) + \mu_1\mathbf{x}_1(k)e(k)\end{aligned} \tag{23}$$

where μ_1 and μ_2 represent the step-size parameters. Note that, since the proposed LMS-SAS algorithm combines the solution of two shorter adaptive filters of length $L_0 = \sqrt{L}$, the stability bounds for μ_1 and μ_2 are usually larger as compared to the corresponding interval for the step-size parameter μ of the conventional LMS counterpart; hence, larger values of μ_1 and μ_2 can be used in the LMS-SAS algorithm, making it possible to achieve higher convergence speed as compared to the conventional LMS.

3.3. NLMS algorithm with symmetric/antisymmetric properties

Considering a similar approach as the one that led to (22)–(23), the update rules of the NLMS algorithm with symmetric/antisymmetric properties (termed here NLMS-SAS) are derived as

$$\widehat{\mathbf{h}}_1(k) = \widehat{\mathbf{h}}_1(k-1) + \frac{\alpha_1\mathbf{x}_2(k)e(k)}{\mathbf{x}_2^{\mathrm{T}}(k)\mathbf{x}_2(k)+\delta_1} \tag{24}$$

and

$$\widehat{\mathbf{h}}_2(k) = \widehat{\mathbf{h}}_2(k-1) + \frac{\alpha_2\mathbf{x}_1(k)e(k)}{\mathbf{x}_1^{\mathrm{T}}(k)\mathbf{x}_1(k)+\delta_2} \tag{25}$$

where α_1 and α_2 are the normalized step-size parameters while δ_1 and δ_2 are the regularization parameters.

3.4. Additional remarks

The main feature of the proposed LMS-SAS and NLMS-SAS algorithms is their ability to operate with shorter filters, as compared with the conventional LMS and NLMS counterparts. In fact, the proposed algorithms combine the solutions of two filters of length L_0, while the conventional LMS and NLMS counterparts update a single adaptive filter of length $L = L_0^2$. Also, the proposed algorithms take into account the specific symmetric or antisymmetric properties of the system impulse response, which are not considered in the conventional LMS and NLMS counterparts. Consequently, improved performance characteristics are expected in this special condition (as supported in Section 4 through numerical simulations). A detailed convergence analysis of the proposed algorithms is not a trivial task due to the connection between $\widehat{\mathbf{h}}_1(k)$ and $\widehat{\mathbf{h}}_2(k)$; hence, this analysis is beyond the scope of the present research work. Nevertheless, we expect that such an analysis would inherit some similarities with the case of the adaptive filters operating with bilinear forms [18, 23].

4. SIMULATION RESULTS

To assess the performance of the proposed algorithms, MC simulations (average of 50 independent runs) are performed for a system identification setup [see (1)] covering four different scenarios. In these simulations, the unknown impulse response $\overline{\mathbf{h}}\,(\mathbf{h}_1, \mathbf{h}_2)$ is obtained from (2), with $\mathbf{h}_1$ containing the first $L_0 = 32$ weights of the echo path model given in the ITU-T G.168 Recommendation [24, Model 1] while $\mathbf{h}_2 = (-0.9)^{l-1}$ for $l = 1, 2, \ldots, (L_0 = 32)$; consequently, the length of $\overline{\mathbf{h}}\,(\mathbf{h}_1, \mathbf{h}_2)$ is $L = L_0^2 = 1024$. Note that both cases resulting from (2) are considered, i.e., symmetric (denoted by $\overline{\mathbf{h}}_+$) and antisymmetric (denoted by $\overline{\mathbf{h}}_-$) impulse responses. The input signal $x(k)$ is either a white Gaussian noise, a correlated signal [which is obtained by filtering a white Gaussian noise through an AR(1) model with a pole at 0.9] [4], or a speech sequence. The system output $y(k)$ is corrupted by an additive white Gaussian noise $w(k)$ such that the signal-to-noise ratio (SNR)[2] is 20 dB. The initialization conditions chosen for the proposed algorithms are $\widehat{\mathbf{h}}_1(0) = L_0^{-1}[1\ \ 1\ \ \ldots\ \ 1]^{\mathrm{T}}$ and $\widehat{\mathbf{h}}_2(0) = [1\ \ \mathbf{0}_{L_0-1}^{\mathrm{T}}]^{\mathrm{T}}$, while for the LMS and NLMS counterparts $\widehat{\mathbf{h}}(0) = \mathbf{0}_L$. The performance metric used in all examples is the normalized misalignment (in dB), defined as

$$\kappa(n) = 10\log_{10}\left[\frac{||\overline{\mathbf{h}}(\mathbf{h}_1,\mathbf{h}_2) - \widehat{\overline{\mathbf{h}}}(k)||^2}{||\overline{\mathbf{h}}(\mathbf{h}_1,\mathbf{h}_2)||^2}\right] \tag{26}$$

which represents the accuracy of the solution provided by the adaptive filter, i.e., the distance between the true impulse response of the system and its estimate. Lastly, aiming to assess the tracking capabilities of the algorithms, an abrupt change of the system is considered in the middle of the adaptation process by shifting the impulse response $\mathbf{h}_1$ to the right by 4 samples while keeping its length unaltered.

Example 1. In this example, the performance of the conventional LMS [4] is compared to the proposed LMS-SAS algorithm. To this end, different step-size values (chosen, within the stability range, to yield the same misalignment in steady state) are used in each algorithm, the system to be identified is $\overline{\mathbf{h}}_+$, and the input signal is taken from a white Gaussian process. Notice from the misalignment curves depicted in Fig. 1 that the LMS-SAS algorithm outperforms the conventional LMS counterpart in terms of the convergence speed and tracking capabilities, when both algorithms are constrained to achieve the same misalignment in steady state. This improved performance is because of the symmetric characteristic of the impulse response and the use of two shorter adaptive filters in the LMS-SAS, instead of a longer one as in the conventional LMS algorithm.

Example 2. Here, the performance of the conventional LMS [4] is compared to the proposed LMS-SAS algorithm for correlated input signals. To this end, different step-size values (chosen to result in the same misalignment in steady state) are used in each algorithm, the system to be identified is $\overline{\mathbf{h}}_-$, and the correlated Gaussian input signal is obtained from an AR(1) process. Fig. 2 illustrates the misalignment curves for this operating scenario. Observe that the improved performance of the LMS-SAS algorithm becomes even more evident for the case of correlated input signals, since the LMS-SAS outperforms the conventional LMS counterpart irrespective of the step-size value considered. Moreover, one verifies in this figure that smaller values of μ_1 and μ_2 reduce the convergence speed of the LMS-SAS, resulting then in lower misalignment in steady state (as also occurs in the conventional LMS).

Example 3. This example aims to assess the performance of both the conventional NLMS [4] and the NLMS-SAS algorithms, which are more robust in terms of selection of the normalized step-size parameter. To this end, different normalized step-size values (chosen to yield the same misalignment in steady state) are used in each algorithm, the system to be identified is $\overline{\mathbf{h}}_+$, and the correlated Gaussian input signal is taken from an AR(1) process. The results obtained are shown in Fig. 3. It can be noticed that smaller values of α_1 and α_2 in

[2]The SNR is defined here as σ_y^2/σ_w^2 with σ_y^2 and σ_w^2 denoting the variances of $y(k)$ and $w(k)$, respectively [according to (1)].

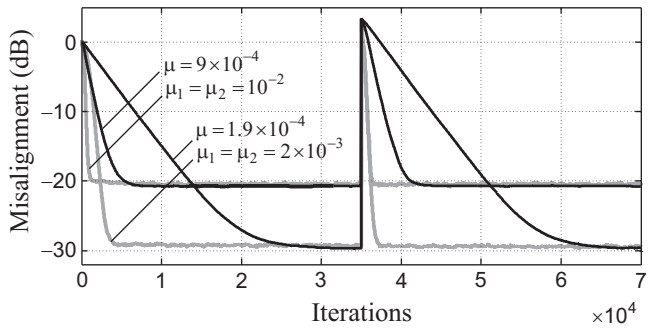

Fig. 1. Example 1. Misalignment of the conventional LMS (dark-ragged lines) and the LMS-SAS (gray-ragged lines) algorithms, considering different step-size values, unknown system impulse response $\overline{\mathbf{h}}_{+}$, and white Gaussian noise as the input signal.

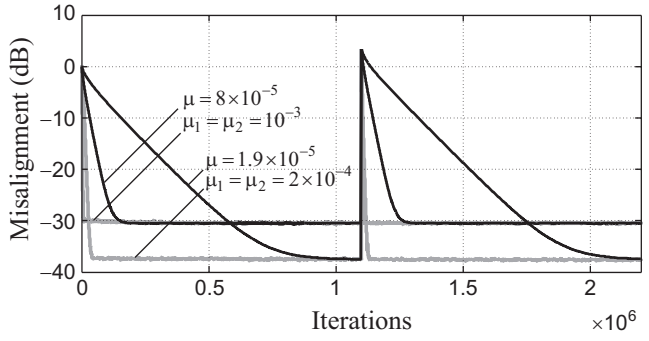

Fig. 2. Example 2. Misalignment of the conventional LMS (dark-ragged lines) and the LMS-SAS (gray-ragged lines) algorithms, considering different step-size values, unknown system impulse response $\overline{\mathbf{h}}_{-}$, and input signal obtained from an AR(1) process.

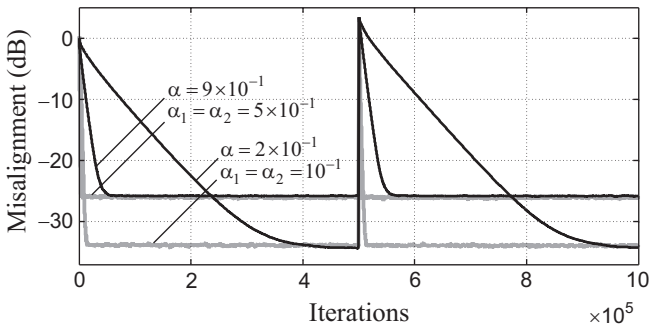

Fig. 3. Example 3. Misalignment of the conventional NLMS (dark-ragged lines) and the NLMS-SAS (gray-ragged lines) algorithms, for different normalized step-size values, unknown system impulse response $\overline{\mathbf{h}}_{+}$, and input signal obtained from an AR(1) process.

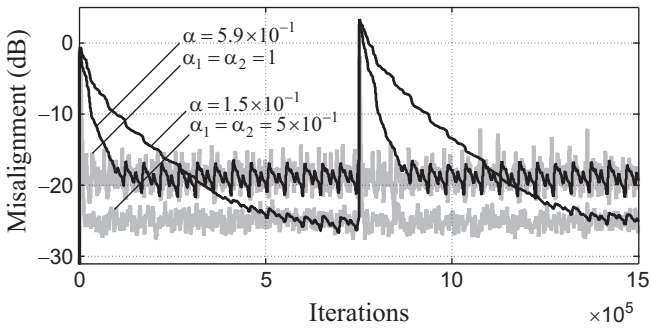

Fig. 4. Example 4. Misalignment of the conventional NLMS (dark-ragged lines) and the NLMS-SAS (gray-ragged lines) algorithms, for different normalized step-size values, unknown system impulse response $\overline{\mathbf{h}}_{-}$, and input signal obtained from a speech sequence (using a single run).

the NLMS-SAS reduce the convergence speed, yielding also lower values of misalignment in steady state (as in the conventional NLMS counterpart). Besides this aspect, one observes from this figure that the NLMS-SAS algorithm using $\alpha_1 = \alpha_2 = 0.5$ outperforms the conventional NLMS operating close to its fastest convergence mode. So, the use of two shorter filters along with the symmetric characteristic of the impulse response results in higher convergence speed for the NLMS-SAS than the conventional NLMS algorithm.

Example 4. In this last example, the robustness of the conventional NLMS and the NLMS-SAS algorithms is assessed vis-à-vis nonstationary input signals. To this end, different normalized step-size values (adjusted to produce the same steady-state misalignment) are used in each algorithm, the system to be identified is $\overline{\mathbf{h}}_{-}$, while the input signal is a speech sequence. The results for this scenario are shown in Fig. 4. Notice that the NLMS-SAS outperforms the conventional NLMS algorithm (in terms of convergence speed and tracking capabilities) even for a nonstationary (speech) input signal. Lastly, it can be highlighted that the enhanced convergence speed of the NLMS-SAS (as opposed to the conventional NLMS) is maintained even when the normalized step-size parameters are halved.

5. CONCLUSIONS

In this paper, LMS-based algorithms were developed exploiting the intrinsic symmetric/antisymmetric properties of the system impulse responses. The proposed LMS-SAS and NLMS-SAS algorithms have been based on a combination of bilinear forms, resulting in the update of two shorter adaptive filters instead of a longer one as occurs in the conventional LMS and NLMS algorithms. Consequently, the proposed algorithms outperform significantly the conventional LMS and NLMS counterparts, in terms of convergence speed and tracking capabilities. Simulation results confirmed the improved performance achieved by the proposed algorithms for different operating scenarios. Further research could address the identification of more general forms of system impulse responses, e.g., using the nearest Kronecker product decomposition and low-rank approximations.

6. RELATION TO PRIOR WORK

In contrast to [9, 17, 18, 23] which consider a multiple-input/single-output (MISO) system identification problem, the development presented here has focused on the use of bilinear forms to represent the input-output relationship of a SISO system whose impulse response owns intrinsic symmetric or antisymmetric properties. In this context, [20] has presented recently an iterative Wiener filter for the identification of such impulse responses, while, in the present research work, we have derived the LMS and NLMS algorithms with symmetric/antisymmetric properties.

7. REFERENCES

[1] J. Benesty and Y. Huang, *Adaptive Signal Processing–Applications to Real-World Problems*. Berlin, Germany: Springer-Verlag, 2003.

[2] A. H. Sayed, *Adaptive Filters*. Hoboken, NJ: John Wiley & Sons, 2008.

[3] P. S. R. Diniz, *Adaptive Filtering: Algorithms and Practical Implementation*, 4th ed. New York, NY: Springer-Verlag, 2013.

[4] S. Haykin, *Adaptive Filter Theory*, 5th ed. Upper Saddle River, NJ: Prentice Hall, 2014.

[5] S. L. Gay and J. Benesty, *Acoustic Signal Processing for Telecommunication*. Boston, MA: Kluwer Academic Publisher, 2000.

[6] J. Benesty, T. Gänsler, D. R. Morgan, M. M. Sondhi, and S. L. Gay, *Advances in Network and Acoustic Echo Cancellation*. Berlin, Germany: Springer-Verlag, 2001.

[7] C. Paleologu, J. Benesty, and S. Ciochină, *Sparse Adaptive Filters for Echo Cancellation*. San Rafael, CA: Morgan & Claypool Publishers, 2010.

[8] J. Liu and S. L. Grant, "Proportionate adaptive filtering for block-sparse system identification," *IEEE/ACM Trans. Audio, Speech, Lang. Process.*, vol. 24, no. 4, pp. 623–630, Apr. 2016.

[9] M. Rupp and S. Schwarz, "A tensor LMS algorithm," in *Proc. IEEE Int. Conf. Acoust., Speech, Signal Process. (ICASSP)*, South Brisbane, QLD, Australia, Apr. 2015, pp. 3347–3351.

[10] L.-M. Dogariu, C.-L. Stanciu, C. Elisei-Iliescu, C. Paleologu, J. Benesty, and S. Ciochină, "Tensor-based adaptive filtering algorithms," *Symmetry*, vol. 13, no. 3, pp. 1–27, Mar. 2021, Identifier: 481.

[11] A. Cichocki, R. Zdunek, A. H. Pan, and S. Amari, *Nonnegative Matrix and Tensor Factorizations: Applications to Exploratory Multiway Data Analysis and Blind Source Separation*. Chichester, UK: Wiley, 2009.

[12] M. Boussé, O. Debals, and L. De Lathauwer, "A tensor-based method for large-scale blind source separation using segmentation," *IEEE Trans. Signal Process.*, vol. 65, no. 2, pp. 346–358, Jan. 2017.

[13] J. Benesty, I. Cohen, and J. Chen, *Array Processing–Kronecker Product Beamforming*. Cham, Switzerland: Springer-Verlag, 2019.

[14] L. N. Ribeiro, A. L. F. de Almeida, and J. C. M. Mota, "Separable linearly constrained minimum variance beamformers," *Signal Process.*, vol. 158, pp. 15–25, May 2019.

[15] M. A. O. Vasilescu and E. Kim, "Compositional hierarchical tensor factorization: Representing hierarchical intrinsic and extrinsic causal factors," in *Proc. ACM Int. Conf. Knowl. Discovery Data Mining (SIGKDD)*, Anchorage, AK, USA, Aug. 2019, pp. 1–9.

[16] M. A. O. Vasilescu, E. Kim, and X. S. Zeng, "Causalx: Causal explanations and block multilinear factor analysis," in *Proc. Int. Conf. Pattern Recognit. (ICPR)*, Milan, Italy, Jan. 2021, pp. 10 736–10 743.

[17] J. Benesty, C. Paleologu, and S. Ciochină, "On the identification of bilinear forms with the Wiener filter," *IEEE Signal Process. Lett.*, vol. 24, no. 5, pp. 653–657, May 2017.

[18] C. Paleologu, J. Benesty, and S. Ciochină, "Adaptive filtering for the identification of bilinear forms," *Digit. Signal Process.*, vol. 75, pp. 153–167, Apr. 2018.

[19] E. V. Kuhn, C. A. Pitz, M. V. Matsuo, K. J. Bakri, R. Seara, and J. Benesty, "A Kronecker product CLMS algorithm for adaptive beamforming," *Digit. Signal Process.*, vol. 111, Identifier: 102968, Apr. 2021.

[20] J. Benesty, C. Paleologu, and S. Ciochină, "On the identification of symmetric and antisymmetric impulse responses," in *Proc. Asilomar Conf. Signals, Syst., Comput.*, Pacific Grove, CA, USA, Oct.-Nov. 2021, pp. 1–5.

[21] C. F. Van Loan, "The ubiquitous Kronecker product," *J. Comput. Appl. Math.*, vol. 123, no. 1, pp. 85–100, Nov. 2000.

[22] J. Benesty, C. Paleologu, and S. Ciochină, "On regularization in adaptive filtering," *IEEE Trans. Audio, Speech, Lang. Process.*, vol. 19, no. 6, pp. 1734–1742, Aug. 2011.

[23] K. J. Bakri, E. V. Kuhn, R. Seara, J. Benesty, C. Paleologu, and S. Ciochină, "On the stochastic modeling of the LMS algorithm operating with bilinear forms," *Digit. Signal Process.*, vol. 122, Identifier: 103359, Apr. 2022.

[24] "ITU-T Recommendation G.168 – Digital Network Echo Cancellers," International Telecommunications Union - Telecommunication Standardization Sector, Geneva, Switzerland, Apr. 2015.